

Amplification and Scintillation Properties of Oxygen-Rich Gas Mixtures for Optical-TPC Applications

L. Weissman^{1†}, M. Gai^{1,2}, A. Breskin³, R. Chechik³, V. Dangendorf⁴,
K. Tittelmeier⁴ and H.R. Weller⁵

1. *Laboratory for Nuclear Science at Avery Point, University of Connecticut,
1084 Shennecossett Rd, Groton, CT 06340, USA.*

2. *Department of Physics, WNSL, Yale University,*

PO Box 208124, 272 Whitney Avenue, New Haven, CT 06520-8124 USA.

3. *Department of Particle Physics, Weizmann Institute of Science, 76100 Rehovot, Israel.*

4. *Physikalisch-Technische Bundesanstalt, 38116 Braunschweig, Germany.*

5. *Department of Physics, Triangle Universities Nuclear Laboratory, Box 90308,
Duke University, Durham, NC 27708, USA.*

Abstract

We studied electron amplification and light emission from avalanches in oxygen-containing gas mixtures. The mixtures investigated in this work included, among others, CO₂ and N₂O mixed with Triethylamine (TEA) or N₂. Double-Step Parallel Gap (DSPG) multipliers and Thick Gas Electron Multipliers (THGEM) were investigated. High light yields were measured from CO₂+N₂ and CO₂+TEA, though with different emission spectra. We observed the characteristic wave-length emission of N₂ and of TEA and used a polymer wave-length shifter to convert TEA UV-light into the visible spectrum. The results of these measurements indicate the applicability of optical recording of ionizing tracks in a TPC target-detector designed to study the cross-sections of the ¹⁶O(γ,α)¹²C reaction, a central problem in nuclear astrophysics.

Keywords: *Optical Readout of gas avalanches, Time Projection Chamber, Thick Gas Electron Multiplier (THGEM), gas amplification, gas scintillation, oxygen-rich counting gas.*

Submitted to JINST, February 23, 2006

[†] Corresponding author: leonid.weissman@uconn.edu

I. INTRODUCTION

This work was motivated by the quest for an oxygen-rich gas mixture for the Optically read out Time Projection Chamber (O-TPC) "target-detector", designed to study the $^{16}\text{O}(\gamma,\alpha)^{12}\text{C}$ reaction in the gamma energy range of 7.9–10.0 MeV [1]. Its time-reversed $^{12}\text{C}(\alpha,\gamma)^{16}\text{O}$ reaction is a fundamental unknown in stellar evolution theory and our experiment will enable determining its cross-section in the a energy range of below 1.2 MeV.

The concept of TPCs was developed in the middle of the 1970s [2] and has been broadly used in particle and nuclear physics [3]. In most applications radiation-induced charged-particle tracks are recorded electronically. Optical avalanche readout systems, on the other hand, present an attractive alternative for low counting-rate applications and for the detection of complex event patterns [4]. The first developments of Optical readout TPC (O-TPC) were: 3D deposited-charge imaging in a calorimeter prototype [5] and single-photon imaging in a UV-sensitive gaseous detector for Cherenkov Ring Imaging (RICH) [6]. The optical readout provides genuine 2D (or 3D) images at a moderate cost. It is decoupled from the detector electrodes and vessel, having the advantages of avoiding electronic pickup noise and of high-voltage decoupling from the readout electrodes. Fast optical sensors (e.g. photomultipliers) can provide trigger signals to the slower optical recording system, usually consisting of a gated Intensified CCD camera (ICCD) [5,7,8]. The optically read out TPC end-cups are usually simple, and consist of cascaded parallel-mesh avalanche multipliers, within which the light emission is higher compared to that in wire structures [4]. Although the O-TPC concept is well established, only a few applications have been published: in the fields of dosimetry [8,9], radiography [10], thermal neutron instrumentation [11], as well as in the experiment for the study of two-proton radioactive decay of the ^{45}Fe nucleus [12]. In [9-11] the authors made use of the GEM (Gas Electron Multiplier [13]) technique.

A major challenge in designing an O-TPC detector is choosing the gas mixture. In addition to the standard requirements of the electron transport parameters for best track quality, the detector gas should also exhibit good light emission (scintillation) properties to provide efficient and accurate optical imaging. Moreover, in cases where the gas serves also as the reaction target, its composition should match the particular application. A common practice is to use admixtures of Triethylamine (TEA) or Tetrakis[dimethylamino]ethylene (TMAE) vapors, which usually added to Ar/hydrocarbon mixtures [4]. These vapors are known for their efficient scintillation properties and were found to yield large avalanche-induced light outputs - up to one photon per avalanche electron [14]. Low photoionization thresholds of TEA and TMAE allowed their use

as “gaseous photocathodes” in UV-photon detectors for Ring Imaging Cherenkov (RICH) devices, including optically read out detectors [6]. However, the use of these vapors often leads to significant complications in detectors and gas-handling systems; e.g. TMAE is very chemically reactive, which causes aging of the detector components. Other gas mixtures, which are simpler to use, were investigated. For example CF_4 was found to emit copious light [15] and has been recently used in O-TPCs [9,12,16]. In an earlier study $\text{Ar} + \text{N}_2(2\%)$ was reported to have comparable light yield to that of $\text{Ar} + \text{TEA}(2\%)$ [17]. Therefore the properties of nitrogen-containing gas mixtures might be of interest for optically read out detectors.

Our goal is the application of an O-TPC detector for the measurement of the cross-section of the $^{16}\text{O}(\gamma,\alpha)^{12}\text{C}$ nuclear reaction [1] at a new generation of gamma-beam facilities such as HIgS [18]. An O-TPC setup is well suited for such studies where the detector, with its counting-gas also serving as the interaction medium for the gamma-beam, is used to measure the signature of very rare reaction products. Via phase-space considerations these data can be converted to provide the cross-section of the time-reversed $^{12}\text{C}(\alpha,\gamma)^{16}\text{O}$ nuclear reaction. The advantages of measuring the inverse reaction are the significantly larger cross-section and the high luminosity of the available gamma-beam. Furthermore, the reaction products, alpha-particles and carbon ions, are expected to be measured and identified with close to 100% efficiency and with reliable background rejection. The experiment is also expected to yield the angular distribution of the reaction products, and thus a partial wave analysis of the reaction cross-sections [1]. As the cross-section value is expected to be very low, the O-TPC gas-mixture, which constitutes the target volume, should be as dense as possible and contain the maximum possible fraction of oxygen.

Several oxygen-rich gas mixtures were studied in this work, with the objective of reaching both high electron multiplication and high avalanche-induced light yields. We investigated parallel-mesh gaseous multipliers, as well as the novel THick Gas Electron Multipliers (THGEM) [19,20] as candidates for the O-TPC end-cup. The possibility of using wave-length shifters (WLS) to shift the emitted UV light into the more practical visible spectral range [12,17] also was considered.

II. EXPERIMENTAL SETUP

The following parameters of different gas mixtures were examined : 1. the total number of emitted photons ("light"); 2. the spectra of emitted light; 3. the total number of avalanche-

induced electrons ("charge"); 4. the energy resolution of the detector; 5. the performance of the electron multiplier structure (grid gap structures and THGEM); and 6. the quality of the track images.

A schematic diagram of the O-TPC detector used to measure gain and light emission is shown in Fig. 1. The detector was filled with gas at a typical pressure of $p=75$ Torr. This choice of pressure is dictated by the track lengths of the reaction products required for an unambiguous identification of the $^{16}\text{O}(\gamma,\alpha)^{12}\text{C}$ reaction. Different gas pressures were also used for studying imaging properties of the optical read out system. A drift region that defines the fiducial volume of the detector was created by two 80% optically transparent wire-mesh electrodes separated by 20 mm. The grids were made of stainless steel wires of $50\ \mu\text{m}$ diameter spaced 0.5 mm apart. The grids defining the drift volume are denoted in Fig. 1 as drift cathode (DC) and drift anode (DA). Typical values of the reduced drift field is $6.5\ \text{V}/(\text{Torr cm})$. Collimated alpha-particles were emitted from a non-spectroscopic gold-coated ^{241}Am radioactive source (mean energy of ~ 4.5 MeV and FWHM of energy distribution of 350 keV). The source was placed below the drift region, irradiating the detector at 45 degrees relative to the drift field lines, as shown in Fig. 1. The range of these 4.5 MeV alpha-particles, at a pressure of 75 Torr, is 10-22 cm, depending on which gas mixture was tested. The primary electrons created in the sensitive volume along the alpha-particle track drift toward the drift anode (DA) and experience two-step multiplication in the Double-Stage Parallel Gap (DSPG) multiplier. The multiplier was defined by the three mesh planes DA, G_1 and G_2 , placed at a 3.2 mm distance from each other (Fig.1). In some other configurations studied here, the electrons were multiplied in a sequence of a THGEM multiplier and a parallel-grid gap. The avalanche multiplication process yields a proportional amount of photons due to excitation of the gas molecules, thus most of the photon emission occurs at the final amplification stage [8,14]. The amounts of avalanche-induced charge and light strongly depend on the values of the electrical fields in the multiplication gaps. The reduced electric field in the amplification gaps was varied between 10 to $65\ \text{V}/(\text{Torr cm})$ and light emission was typically observed at reduced-field values higher than $20\ \text{V}/(\text{Torr cm})$. The charge produced by the avalanche was collected on G_2 and was amplified by a calibrated charge-sensitive preamplifier and a linear spectroscopy amplifier. The signals were analyzed using a PC-based multichannel analyzer (Amptek, MCA8000A). The emitted photons were detected by a UV-sensitive Photonis XP-2020Q photomultiplier (PMT). The PMT was placed 44 mm from the light emission region, behind a quartz view port. It collected the avalanche-induced light within a

solid angle of 6.5% of 4p. The signal from the PMT anode was amplified by a linear spectroscopy amplifier and analyzed using the same MCA.

A second data acquisition (DAQ) system was also used for analyzing the charge and light spectra. This CAMAC-based DAQ (KMAX by Sparrow Inc.) incorporated an eight-channel ORTEC ADC, AD811. The use of this DAQ system allowed one to establish 2D charge versus light correlation plots.

Typical avalanche-induced charge (electron yield distribution) and light (photoelectron yield distribution) spectra are shown in Fig. 2. Note that the observed FWHM (of ~ 20 %) of the distributions was due to dispersion in the energy loss of alpha-particles. This was partially due to the initial alpha-particle energy distribution, but mostly because of the geometrical variations of the track lengths. These variations were associated with insufficient collimation of the source. A significantly improved energy resolution was recorded in a further study performed with a spectroscopic-quality source (see below).

The electron charge amplification was determined from the ratio of the measured charge (i.e. the number of avalanche electrons), to the calculated number of primary electrons produced in the drift region. The latter was calculated for each gas mixture using the stopping power tables [21] and the known W-values – the mean energies of formation of an electron-ion pair. The total number of photons emitted into 4p was calculated from the number of photoelectrons measured at the PMT photocathode multiplied by its wave-length dependent quantum efficiency, as provided by the manufacturer, and the calculated solid-angle of the PMT. The number of photoelectrons produced in the PMT photocathode was determined from the PMT pulse-height spectrum (Fig. 2) normalized to the single-photoelectron peak. This peak was obtained from the thermal-emission spectrum at high PMT bias voltages of -2.1-2.3 kV and was corrected to the PMT gain difference at the operating voltages of -1.0-1.4 kV. The measured PMT multiplication curve was used for this correction. The uncertainties in the PMT calibration procedure and in the quantum efficiency of the PMT cathode (up to 30% according to the manufacturer) are the main factors contributing into the overall systematic uncertainty in the determination of absolute light yield. This overall uncertainty may amount to up to 50%. The number of photons per electron, ph/e , in the avalanche was readily deduced from measured charge and light.

Transmission filters were placed in front of the PMT in the measurements of the light emission spectra from the mixtures of interest (see below). A set of transmission filters with cutting edges at the wavelengths (λ_c) of 280, 290, 305, 320, 335, 345, 360, 375, 400, 420, 435, 455, 475, 485, 530, 580 and 630 nm was used for this purpose.

High-purity (99.999%) gases were used in all measurements. The detector was operated in continuous gas-flow mode using the gas handling system shown in Fig. 3. The system allows for mixing up to three different gases. The partial pressures of the gas components were set by mass-flow controllers and the overall pressure in the detector was controlled by a capacitive pressure gauge. All parameters of the gas system were set by a MKS146 controller (MKS Instruments Inc.). TEA vapors could be added by bubbling the mixed gas through a reservoir filled with TEA liquid. A cold trap mounted on the pump (Fig. 3) eliminated TEA vapor contamination.

The investigated oxygen-rich gas mixtures were based on carbon dioxide (CO₂) and nitrous oxide (N₂O or “laughing gas”). Neither CO₂ nor N₂O exhibit light emission compatible with optical readout systems sensitive to the UV-to-visible range. Thus other efficient gaseous light emitters, like TEA or TMAE, must be added. The TEA light emission spectrum is centered around 280 nm [22] and requires the use of expensive UV optics. TMAE emits visible light peaking at 480 nm [23], which is compatible with standard optical elements. However, TMAE has high chemical reactivity and low vapor pressure[14], requiring heating of the detector and gas system to rather high temperatures in order to reach a light output comparable to TEA. Therefore only the addition of TEA vapors was practiced in this work. The partial pressure of TEA vapor was controlled by varying the temperature of the liquid in the bubbler. The dependence of TEA vapor pressure on temperature (T) in the applicable temperature range is described by the empirical equation: $p = 52.0 \times e^{(4100 \times (1/293 - 1/T(K)))}$ Torr [24].

A different experimental setup was used for recording images of alpha-particle tracks. The detector and the optical readout system are shown in Fig. 4. The electrodes of the imaging O-TPC had a similar geometry to the one presented in Fig. 1, thus its performance is expected to be the same. A non collimated ²⁴¹Am source was placed to the side of the drift volume, so the tracks were perpendicular to the drift field. A small parallel-plate proportional detector (PPAD) was placed opposite of the alpha-particle source, providing the event trigger for the optical read out chain. Thus, only alpha-particles traversing the whole sensitive volume were registered. Three guard rings biased by a resistive chain were placed between the drift anode and cathode, thus ensuring the homogeneity of the drift field. The ionization electrons produced along the alpha-particle tracks drifted towards the DA. The avalanche-induced light produced in the last multiplication stage was detected by the optical read out system. A quartz UV lens with a focal length of 150 mm and an aperture of F=2.5 focused the light onto the photocathode of an Image Intensifier (Proxifier BV 2562) coupled to a CCD camera [8]. The optical efficiency of the system was estimated to be 4×10^{-4} , and the quantum efficiency of the photocathode was 0.2. This

yielded an effective photon detection efficiency of 8×10^{-3} . The image intensifier was gated by a high voltage (HV) pulse, which was initiated by the PPAD alpha-particle trigger. The CCD analog output signal was digitized by a 12 bit PCI digitizer board (Spectrum MI 3025). After careful CCD background subtraction, track images with a 10 bit useful dynamic range were obtained.

III. EXPERIMENTAL PROCEDURES AND RESULTS

A. Measurements of "charge" and "light" yields

During the initial search for the optimal gas, we performed numerous short tests with various gas mixtures using the setups shown in Fig. 1 and Fig. 4. The tested gases and gas mixtures included pure CO₂, pure N₂O, pure O₂, CO₂+TEA, N₂O+TEA, CO₂+N₂, N₂O+N₂, CO₂+CF₄, CO₂+isobutane and CO₂+O₂. Gas mixtures containing O₂ did not exhibit sufficient gain and did not allow for stable operation of the detector. Pure CO₂ and N₂O gases did not exhibit sufficient light yields in the UV-to-visible spectral range. In these preliminary tests the best results were obtained with CO₂ and N₂O mixed with TEA or N₂. Hence, the detailed systematic measurements were performed only for CO₂+N₂, N₂O+N₂ and CO₂+TEA gas mixtures.

Electron multiplication and light emission were measured while varying the electric fields in the two multiplying gaps as described in the previous section (Fig.1). During the measurements the electric field in the first gap (between grids DA and G₁) was kept at the highest possible value below discharge, while the field in the second gap (between grids G₁ and G₂) was varied. The results of the measurements are presented in Fig. 5. The concentrations of N₂ and TEA in the mixtures are indicated in the figure. The TEA concentrations corresponded to the TEA bubbler temperatures of -4, 5 and 15 °C. The summary of the maximum attainable gains and numbers of emitted photons as a function of N₂ or TEA concentrations is provided in Fig. 6.

As shown in Fig. 5, the ph/e ratio does not decrease by less than a factor of 2 with the increase of the multiplication gain by two orders of magnitude. Hence, the amount of light is essentially proportional to the charge multiplication. This behavior is different from the one usually observed in noble-gas mixtures, where the ph/e ratio decreases by an order of magnitude over a similar multiplication range [12,17]. This phenomenon was explained by a decrease of the excitation cross-sections and an increase of the ionization probability with increasing field values [17]. One can observe from Fig. 5 that the photon-to-electron ratios are similar for the CO₂+N₂ and N₂O+N₂ mixtures with the same N₂ concentrations. However, the use of CO₂+N₂ is more favorable since it allows for the application of higher electric fields, resulting in higher

multiplication factors and higher light yield. Taking into account the higher oxygen content of CO₂, it is clear that CO₂+N₂ is more suitable for the proposed experiment [1] than N₂O+N₂. Although the ph/e ratio for CO₂+N₂ mixtures are somewhat lower than for the corresponding CO₂+TEA mixtures, the charge multiplication factors are higher for the first. Therefore, the absolute maximum number of emitted photons are comparable for these two cases as shown in Fig. 6.

The ph/e ratio for CO₂+N₂ increases linearly with N₂ concentration. However, the maximum charge multiplication factor decreases with N₂ concentration, most likely because of the lower breakdown voltages of N₂ [25]. Therefore, an increase of the N₂ concentration beyond 50% leads to a decrease of the total number of emitted photons (Fig. 6). In fact, the relatively low concentrations of N₂, (e.g. 10%) results in the maximum photon yields of approximately 10⁷ photons per alpha-particle track. This is very well suited to the objective of maximizing the oxygen content in the gas mixture for the planned experiment [1].

B. Measurement of light emission spectra

The light emission properties of the two best oxygen-containing mixtures, CO₂+N₂ and CO₂+TEA, were investigated. Light-emission spectra of CO₂+N₂(10%) and CO₂+TEA(18%) mixtures were measured by utilizing the set of transmission filters (see above). Light distribution spectra similar to those shown in Fig. 2 were collected for each of the filters placed in front of the PMT. All other conditions (voltages, pressure, gas mixture composition) were kept identical. The measured pulse-height centroids are proportional to the number of transmitted photons with wavelengths higher than the cutting edge of the corresponding filter, $\lambda > \lambda_s$. The difference between the photon yields measured in successive exposures with different filters allowed us to derive the emission spectra. The quantum efficiency of the PMT bialkali photocathode, which is almost constant within the investigated spectral range, was also taken into account. The deduced emission spectra are shown in Fig.7.

As pointed out in [22], the emission spectra of noble gases mixed with TEA are dominated by the TEA emission independently of the noble-gas used. The results of our measurements show that the CO₂+TEA mixture has similar spectral characteristics with dominant peak at 280 nm (Fig. 7a). Asymmetric emission bands, of up to 350 nm, were attributed to the radiative deexcitation of the excited TEA molecules [22]. In addition, we repeated the measurements using a polymer Wave Length Shifter (WLS) of the same type as used in [12]. The WLS foil was made of polystyrene doped with dyes. The spectrum measured with the WLS is shown in

Fig. 7a. The WLS shifted the TEA light into the spectral range centered at about 380 nm; however with considerable photon losses.

The light emitted from avalanches in the $\text{CO}_2+\text{N}_2(10\%)$ mixture is shown in Fig. 7b. Most of the emitted light corresponds to the 337 nm N_2 line. However, a significant amount of light is emitted at longer wave lengths (377 and 391 nm lines of N_2) which approach the visible spectral range. The spectrum of nitrogen fluorescence induced by alpha-particle excitation of pure nitrogen gas [26] is shown for comparison in Fig. 7b. The light emission of N_2 is in the soft UV near the visible spectral range. This light emission is beneficial for most applications when compared to the TEA light emission, making possible the use of standard optics.

C. Measurement of energy resolution

The energy resolution of the O-TPC detector is of importance for rejecting anticipated background events in the future experimentation [1]. The data shown in Fig. 2 were obtained without optimization of the energy resolution. In these measurements, variations of the alpha-particle paths within the drift and multiplication regions led to a large spread in the deposited energy. On the other hand, the spread of the energy of alpha-particles emerging from the gold-plated source was founded to be 8 % (FWHM).

In order to measure the energy resolution of the O-TPC, we used a spectroscopic ^{241}Am source ($E_a = 5.49$ MeV). A 3 mm diameter collimator was placed next to the source and a second, 1 mm diameter, collimator was placed at a 25 mm distance from the source. The source was mounted to the side of the drift volume, and the collimated alpha-particles impinged perpendicular to the drift field. The CAMAC-based DAQ system (see above) was used in these measurements.

Typical charge and light spectra and a two-dimensional correlation spectrum are shown in Fig. 8. The spectra were taken in $\text{CO}_2+\text{N}_2(10\%)$ at 75 Torr. The voltages on DC, DA, G_1 and G_2 electrodes were -2.2, -1.2, 0 and 1.75 kV respectively. These data exhibit good energy resolution: 8.3% (FWHM) for the charge spectrum and 9.0% (FWHM) for the light spectrum. The light-to-charge correlation spectrum presented in Fig. 7c demonstrates the proportionality between charge and lights. The energy resolution of the O-TPC proposed for the $^{16}\text{O}(\gamma,\alpha)^{12}\text{C}$ experiment is expected to be better due to complete stopping of alpha-particles and carbon ions in a larger O-TPC volume. For example, an energy resolution of 2 % was obtained with an O-TPC in [16] where the alpha-particles were stopped within the drift volume of the detector.

D. Optical imaging of alpha-particle tracks

Images of the alpha-particle tracks were acquired with the imaging O-TPC viewed by an intensified CCD camera, in a setup described in detail in [8] and in the previous section (Fig. 4).

A typical image of an alpha-particle track taken in a $\text{CO}_2+\text{N}_2(10\%)$ mixture at 75 Torr is shown in Fig. 9. The energy loss of the alpha-particles in the sensitive volume is approximately 1.0 MeV. The visible part of this track was 90 mm long. The applied voltages on the DC, DA, G_1 and G_2 electrodes were -1900 V, -800 V, +900 V and +2000 V, respectively. This image was taken at the relatively low multiplication value of approximately 10^3 , corresponding to 4.3×10^6 photons emitted in 4p and 340 photoelectrons produced in the photocathode of the image intensifier. The latter number was obtained by multiplying the number of photons emitted in 4p by the total detection efficiency of the optical system (8×10^{-5} , see above). As seen in Fig. 6 the detector gain and the total number of avalanche-emitted photons can be increased by an order of magnitude for the $\text{CO}_2+\text{N}_2(10\%)$ mixture.

Image properties of CO_2+TEA mixtures were also investigated. For example, track images were optically recorded in 27 Torr of CO_2+TEA . The liquid TEA was kept at -5°C , yielding a $\text{CO}_2+\text{TEA}(50\%)$ mixture. Unlike in $\text{CO}_2+\text{N}_2(10\%)$, we observed "halo" photons around the alpha-particle tracks, as shown Fig 10a. Images taken with prompt (400 ns) and delayed HV gate pulses to the image intensifier are shown in Fig. 10b and Fig. 10c, correspondingly. The delayed emission of the halo photons clearly indicates that they were emitted by a secondary process. It suggests a photon feedback mechanism, where photons from the primary avalanche were reabsorbed in the drift region and induced further ionization electrons. Since re-absorption occurred within a certain volume around the primary avalanche, these secondary electrons led to secondary avalanches that were scattered around the primary ones. Note that such a phenomenon was not observed for the $\text{CO}_2+\text{N}_2(10\%)$ gas mixture or for the pure TEA vapor [8]. Therefore, the observed photon feedback is not associated with photo-effects on the electrodes or on the walls, but is a specific feature of the $\text{CO}_2 + \text{TEA}$ mixtures.

E. Measurements with Thick GEM multipliers

Following the successful implementation of O-TPC detectors with GEM-based light-emitting multipliers [10,11,16] we investigated the light emission properties of the simpler Thick Gas Electron Multipliers (THGEM) [19,20,27,28]. In these hole-multipliers, the avalanche is confined to the holes resulting in photon-feedback suppression. Two series of 10 cm diameter THGEMs (Print Electronics [29]), referred below as THGEM A and THGEM B, were produced

from double-sided copper clad G-10 circuit boards of thicknesses 0.4 mm (A) and 1.6 mm (B) respectively. Other THGEM dimensions are presented in Table 1 and a photograph of a typical THGEM used in this work is shown in Fig. 11. The copper was etched around the hole's rim to reduce the probability of discharges at high voltages [19,20]. The leakage currents across the THGEMs were measured in ambient air as a function of the applied voltage. Those yielding the lowest leakage current (~ 1 nA at 1 kV) were chosen for the tests.

The THGEM was installed in the O-TPC detector replacing the DSPG multiplier. One side of the THGEM was kept at ground potential and was used as a drift anode, as shown in the insert of Fig. 12. A grid electrode, G_1 , was placed 3.2 mm downstream from the THGEM as an optional second amplification and scintillation stage (Fig.12, insert). The amplified charge could be collected on the THGEM or on G_1 . The detector was operated in $\text{CO}_2+\text{N}_2(10\%)$ mixture at 75 Torr. The reduced electric field in the drift volume was similar to the field in the previous measurements (6.5 V/(cmTorr)). In the first test the charge was collected on the THGEM anode while the voltage on the G_1 electrode was kept at ground potential, providing a strong reverse field and full charge collection. The multiplication gains as a function of the applied voltage measured with THGEM A and B are shown in Fig. 12. For the maximum applicable voltages, prior to discharge across the THGEM, we measured gains of $1-1.5 \times 10^3$. Cascading two THGEM elements separated by a 1 cm gap did not increase the total gain beyond 3×10^3 at any possible combination of the THGEM voltages. This suggests that the space charge limit of the gain was reached at least in one hole of the second THGEM at the present conditions. The somewhat lower gains of the THGEM compared to the ones obtained with the DSPG configuration is the subject of further investigation.

The dependence of ph/e ratios as a function of the multiplication gain is shown in Fig. 13. As in the case of DSPG multiplier, the ratios are almost independent of the voltage across the THGEM. However, they are consistently lower than those obtained with two-grid multipliers for the same $\text{CO}_2+\text{N}_2(10\%)$ gas mixture (see Fig. 13). In addition, the ph/e ratios observed for the thicker THGEM B are almost a factor of two lower than those obtained from THGEM A. This suggests either geometrical blocking of the light within the holes, or implies that the scintillation process is less intense in the confined volume. The ph/e ratio in the modified configuration, with an additional amplification process taking place in the gap between the THGEM and the G_1 , is also shown in Fig. 13. In this mode the voltage across the THGEM B was fixed at the maximum value (~ 1.4 kV) and the amplification field in the THGEM- G_1 gap varied while the avalanche

charge was collected on the G_1 grid. In this configuration a higher ph/e ratio was measured at the highest applicable voltages (Fig. 13).

IV. SUMMARY AND DISCUSSION

We studied the properties of oxygen-rich gas mixtures. The gases investigated primarily involved CO_2+N_2 , $\text{N}_2\text{O}+\text{N}_2$ and CO_2+TEA mixtures. CO_2+N_2 and $\text{N}_2\text{O}+\text{N}_2$ gas mixtures were found to exhibit good light-emission yields, when compared to CO_2+TEA mixtures. While the ph/e ratios of CO_2+N_2 and $\text{N}_2\text{O}+\text{N}_2$ mixtures were similar, the maximum amplification gain and total light yield were significantly higher in the case of CO_2+N_2 . In addition, CO_2+N_2 contains twice as much oxygen. The maximum number of photons emitted in the corresponding CO_2+N_2 and CO_2+TEA mixtures were comparable. Thus, the observed high light emission of nitrogen-containing mixtures confirms the results reported almost two decades ago [17].

Light emission by CO_2+TEA at a wave length of 280 nm requires the use of rather expensive UV optics or the use of wave length shifters. However, to follow the WLS option in the proposed O-TPC, a more elaborate investigation is required. The wavelength of the light emitted by the CO_2+N_2 is in the soft UV, near visible range. This is more favorable for the design of an economical optical system.

The energy resolution of the O-TPC detector with the $\text{CO}_2+\text{N}_2(10\%)$ mixture was found to be 8-9 % (FWHM). In the planned experiment the energy resolution of the O-TPC is expected to be better due to the complete stopping of alpha-particles and carbon ions in the drift volume. The obtained energy resolution is sufficient to remove the anticipated background events in the proposed $^{16}\text{O}(\gamma,\alpha)^{12}\text{C}$ experiment.

Good quality images of alpha-particle tracks were obtained in the $\text{CO}_2+\text{N}_2(10\%)$ mixture using the prototype O-TPC detector. These images did not exhibit the photon feedback effect, as for example those obtained from the CO_2+TEA mixture. In the proposed experiment [1] we expect the alpha-particles originating from the $^{16}\text{O}(\gamma,\alpha)^{12}\text{C}$ reaction to lose between 1.0 and 1.8 MeV in the drift region of the O-TPC. The anticipated optical system will have a total detection efficiency of $\sim 1.4 \times 10^{-4}$, which is higher than the efficiency of the system used in this work. This estimation is based on: 1. $30 \times 30 \text{ cm}^2$ active area of the TPC detector (object size); 2. an image intensifier with a cathode diameter of 40 mm (image size); 3. quantum efficiency of the image intensifier of 0.2; and 4. a lens with aperture of $F=1.1$ and focal length of 150 mm. In the planned experiment the energy deposited by the photodisintegration products will be similar to the energy loss of alpha-particles in the present tests. Compared to the conditions at which the image in Fig.

9 was taken the gain and light outputs can be increased by an order of magnitude. All these facts ensure that a similar or even better quality of tracks could be achieved in the experiment.

Thus, it can be concluded from our studies, that $\text{CO}_2+\text{N}_2(10\%)$ is a well suited gas mixture for the planned experiment. Gas mixtures containing nitrogen have many advantages over commonly used mixtures with photosensitive vapors, and may find broader applications in the field of gas detectors.

Further research is needed for evaluating the best light-emitting electron multiplier. The accent should be on maximal light yield, energy resolution, lack of secondary avalanches (halo) and track quality. The highest gains of the order of 10^4 were achieved with the DSPG and THGEM plus grid configurations. The somewhat lower charge and light yields obtained with THGEMs will be address in the future.

V. ACKNOWLEDGEMENTS

The authors acknowledge the help of Mr. M. Klin and Mrs. A. Raanan of the Weizmann Institute, for preparing the gas system and for performing preliminary light-emission measurements. The imaging O-TPC and its read out and data analysis system as well as the detector setup for the light and charge measurements, were made by Dr. G. Laczko, formerly at PTB, Braunschweig. The research was funded in part by TUNL at Duke University, the US department of energy grant number DE-FG02-94ER40870, the Benozio Center for High-Energy Research at the Weizmann Institute, the Israel Science Foundation - project 151/01 and by the Yale-Weizmann Collaboration, ACWIS, New-York. L. Weissman is grateful to Mr. T. Kading for revision of the manuscript. A. Breskin is the W. P. Reuther Professor of Research in the Peaceful use of Atomic Energy.

References:

- [1] M. Gai, A. Breskin, R. Chechik, V. Dangendorf and H. Weller; APH A, Heavy Ion Physics **25**, (2006) in press, and nucl-ex/0504003.
- [2] J.N. Marx and D.R. Nygren; Physics Today, 31,#10 (1978) 46.
- [3] G. Charpak, Nucl. Instr. Meth. **A217** (1983) 5.
- [4] A. Breskin, Nucl. Instr. Meth. **A454** (2000) 26 and references therein.
- [5] P. Fonte, A. Breskin, G. Charpak, W. Dominik and F. Sauli; Nucl. Instr. And Meth. **A283**, (1989) 658.
- [6] A. Breskin, R. Chechik, Z. Fraenkel, D. Sauvage, V. Steiner, I. Tserruya, G. Charpak, W. Dominik, J.P. Fabre, J. Gaudaen, F. Sauli, M. Suzuki, P. Fischer, P. Glässel, H. Ries, and H.J.Specht, Nucl. Instrum. Methods **A273** (1988) 798.
- [7] A. Breskin, R. Chechik and D. Sauvage; Nucl. Instr. and Meth. **A286** (1990) 251.
- [8] U. Titt, A. Breskin, R. Chechik, V. Dangendorf, H. Schmidt-Boecking, H. Schuhmacher; Nucl. Instr. and Meth. **A416** (1998) 85.
- [9] S. Fetal, C.W.E. van Eijk, F. Fraga, J. de Hass, R. Kreuger, T.L. van Vuure, J.M. Schippers; Nucl. Instr. and Meth. **A513** (2003) 42.
- [10] F. A. F. Fraga, L. M. S. Margato, S. T. G. Fetal, M. M. F. R. Fraga, R. Ferreira Marques and A. J. P. L. Policarpo.; Nucl. Instr. and Meth. **A471** (2001) 125.
- [11] G. Manzin, B. Guerard, F.A.F. Fraga and L.M.S. Margato; Nucl. Instr. and Meth. **A535** (2004) 102.
- [12] M. Cwiok, W. Dominik, Z. Janas, A. Korgul, K. Miernik, M. Pfuetzner, M. Sawicka and Wasilewski; to be published in 2004 IEEE Nuclear Science Symposium Conference Record, 16-22 October, 2004, Rome.
- [13] F. Sauli; Nucl. Instr. and Meth. **A386** (1997) 531.
- [14] D. Sauvage, A. Breskin and R. Chechik; Nucl. Instr. and Meth; **A275** (1989) 351.
- [15] A. Pansky, A. Breskin, A. Buzulutskov, R. Chechik, V. Elkind and J. Va'vra; Nucl. Instr. and Meth. **A354** (1995) 262.
- [16] L.M.S. Margato, F.A.F. Fraga, S.T.G. Fetal, M.M.F.R. Fraga, E.F.S. Balau, A. Blanco, R. Ferreira Marques and A.J.P.L Policarpo; Nucl. Instr. and Meth. **A535** (2004) 231.
- [17] G. Charpak, W. Dominik, J. P. Fabre, J. Gaudaen, F. Sauli and M. Suzuki; Nucl. Instr. and Meth. **A269** (1988) 142.
- [18] V. N. Litvinenko, B. Burnham, M. Emamian, N. Hower, J. M. J. Madey, P. Morcombe, P.G. O'Shea, S. H. Park, R. Sachtschale, K. D. Straub, G. Swift, P. Wang, and Y. Wu, R. S. Canon, C. R. Howell, N. R. Roberson, E. C. Schreiber, M. Spraker, W. Tornow, and H. R. Weller, I. V. Pinayev, N. G. Gavrillov, M. G. Fedotov, G. N. Kulipanov, G. Y. Kurkin, S. F. Mikhailov, V. M.

- Popik, A. N. Skrinsky, and N. A. Vinokurov, B. E. Norum, A. Lumpkin and B. Yang; Phys. Rev. Lett. **78**, (1997) 4569.
- [19] R. Chechik, A. Breskin, C. Shalem, D. Mormann; Nucl. Instr. and Meth. **A535** (2004) 303.
- [20] R. Chechik, A. Breskin, C. Shalem; Nucl. Instr. and Meth. **A553** (2005) 35.
- [21] J. Ziegler; SRIM program, <http://www.srim.org>.
- [22] M. Suzuki, P. Strock, F. Sauli and G. Charpak; Nucl. Instr. and Meth. **A254** (1987) 556.
- [23] G. Charpak, W. Dominik, J.P. Fabre, J. Gaudaen, V. Peskov, F. Sauli, M. Suzuki, A. Breskin, R. Chechik and D. Sauvage; IEEE Trans. Nucl. Sci. **NS-35** (1988) 483.
- [24] R. Arnold, Y. Giomataris, J. L. Guyonnet, A. Racz, J. Sguinot, T. Ypsilantis; Nucl. Instr. and Meth. **A314** (1992) 465.
- [25] Y. Qiu, Y.F. Liu, A. Sun and E. Ku_el; J. Phys. **D21** (1988) 208.
- [26] T.D. Strickler and E.T. Arakawa; Journ. Chem. Phys. **41** (1964) 1783.
- [27] C.K. Shalem, R. Chechik, A. Breskin and K. Michaeli, physics/0601115; Nucl. Instr. and Meth. A in press
- [28] C.K. Shalem, R. Chechik, A. Breskin, K. Michaeli and N. Ben-Haim; physics/0601119; Nucl. Instr. and Meth. A in press
- [29] Print Electronics Inc., Rishon Le Zion, Israel, interdes@isdn.net.il.

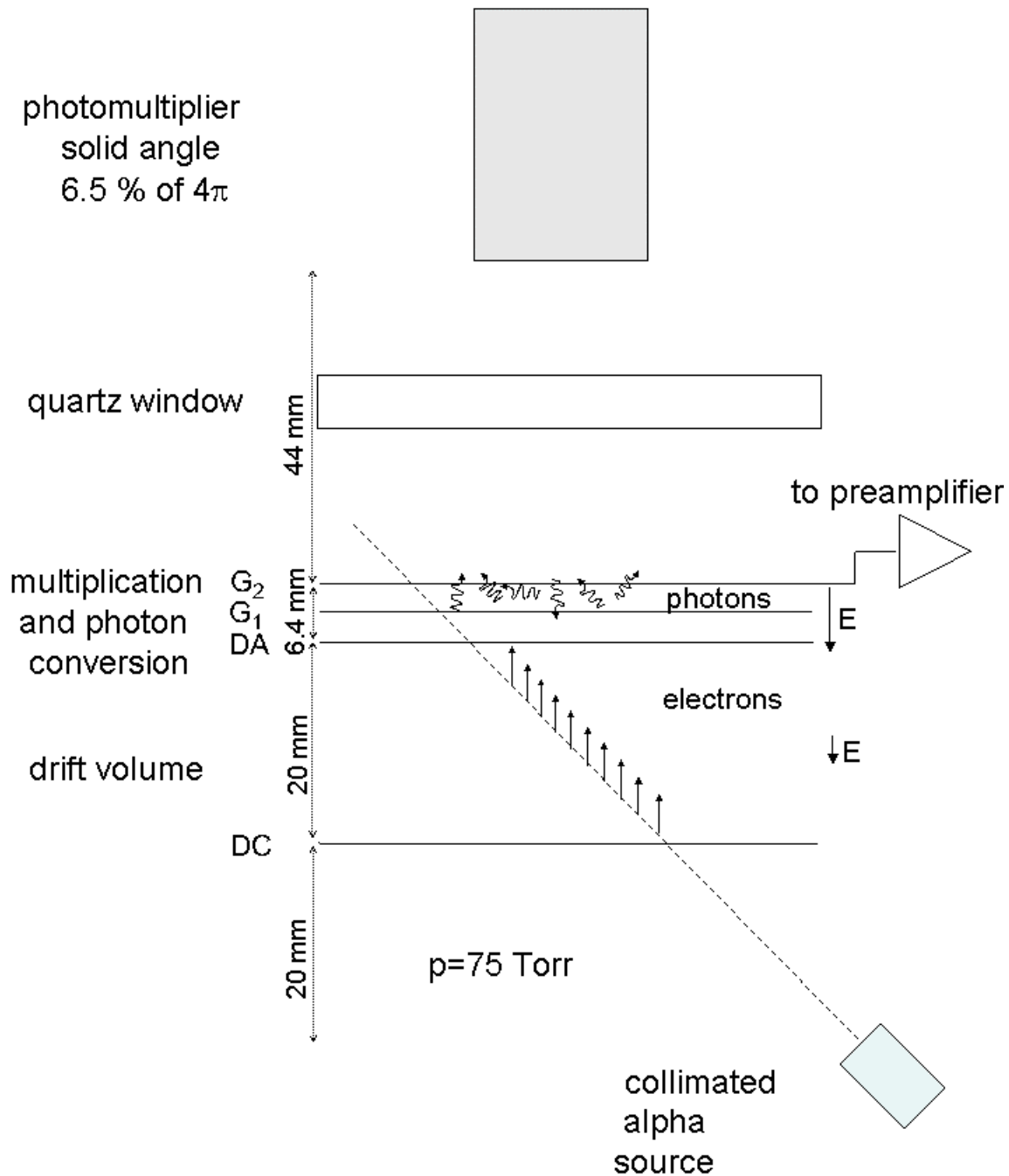


FIG. 1: Schematic diagram of the O-TPC equipped with a Double-Stage Parallel Gap (DSPG) multiplier, for measurements of charge and light yields in various gases.

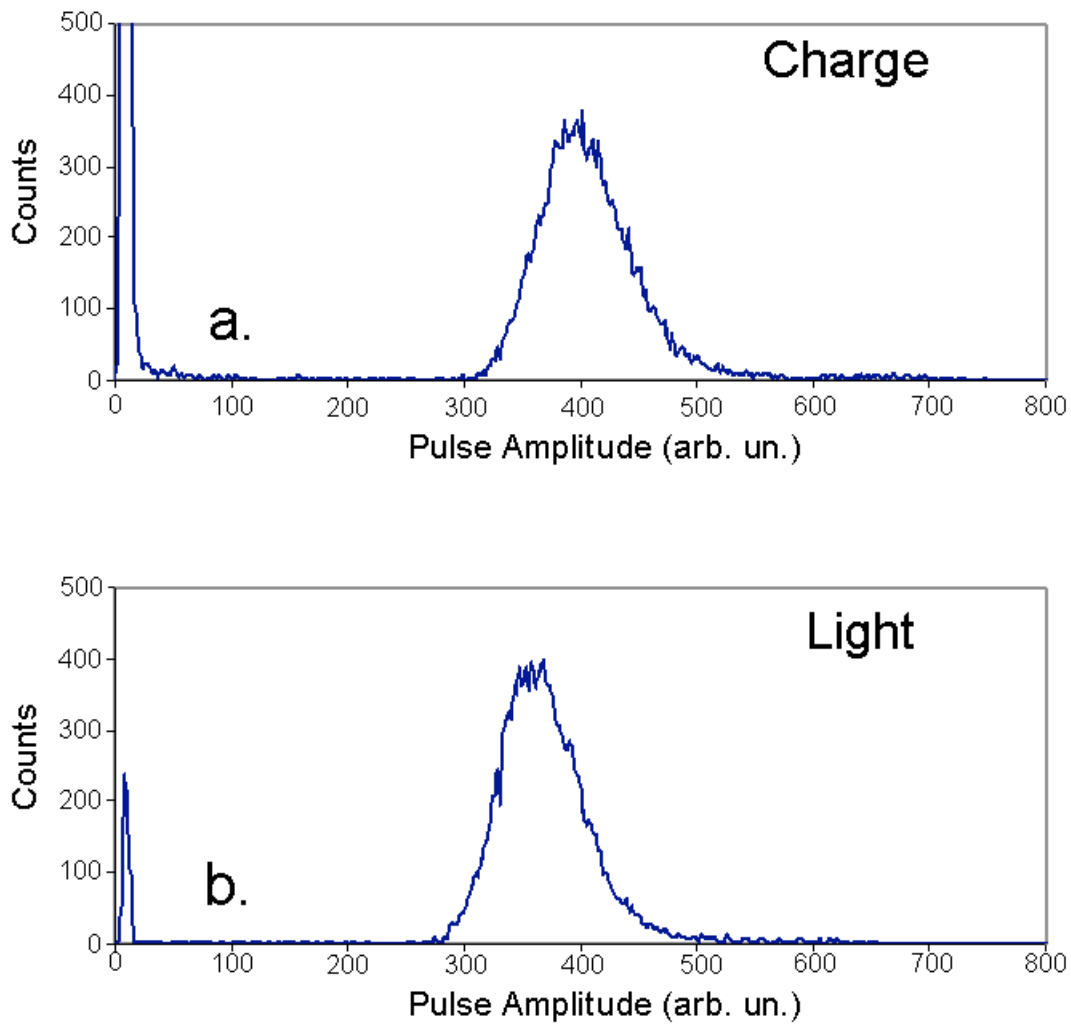


FIG. 2: Typical collected charge (a) and light (b) spectra emitted by a $\text{CO}_2+\text{N}_2(10\%)$ gas mixture. The broad peaks (FWHM approx. 20%) are due to the large distribution of the energy loss of alpha-particles emanating at different angles and having different track length, in the sensitive volume.

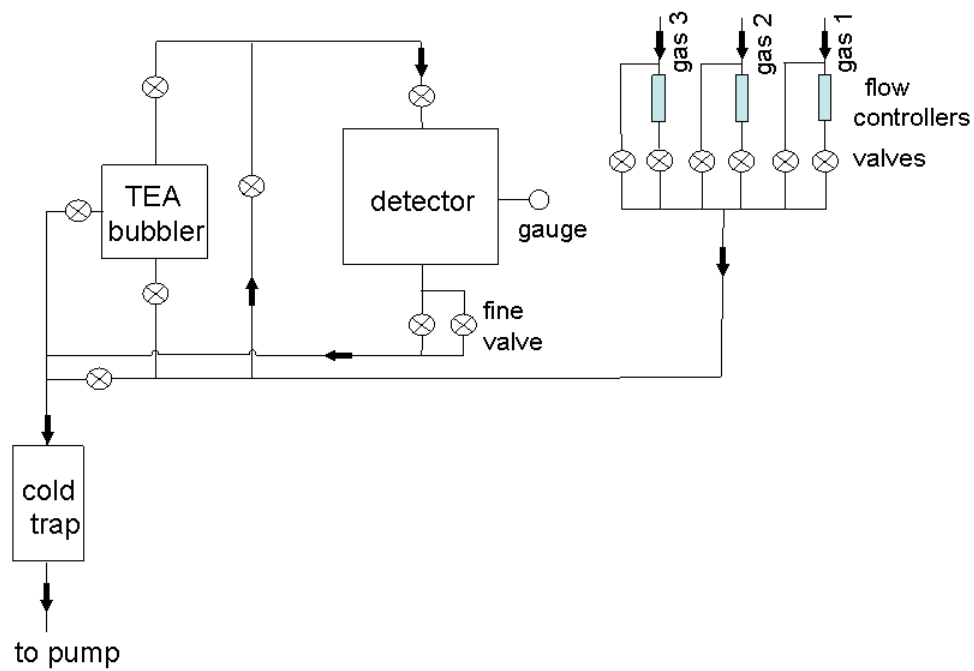


FIG. 3: Schematic diagram of the gas handling system.

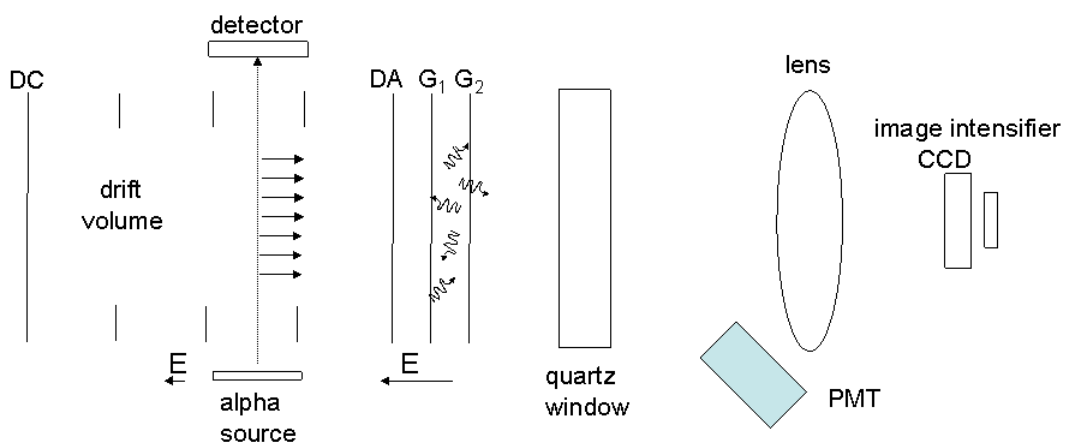


FIG. 4: Schematic diagram of the O-TPC used for recording the tracks of alpha-particles.

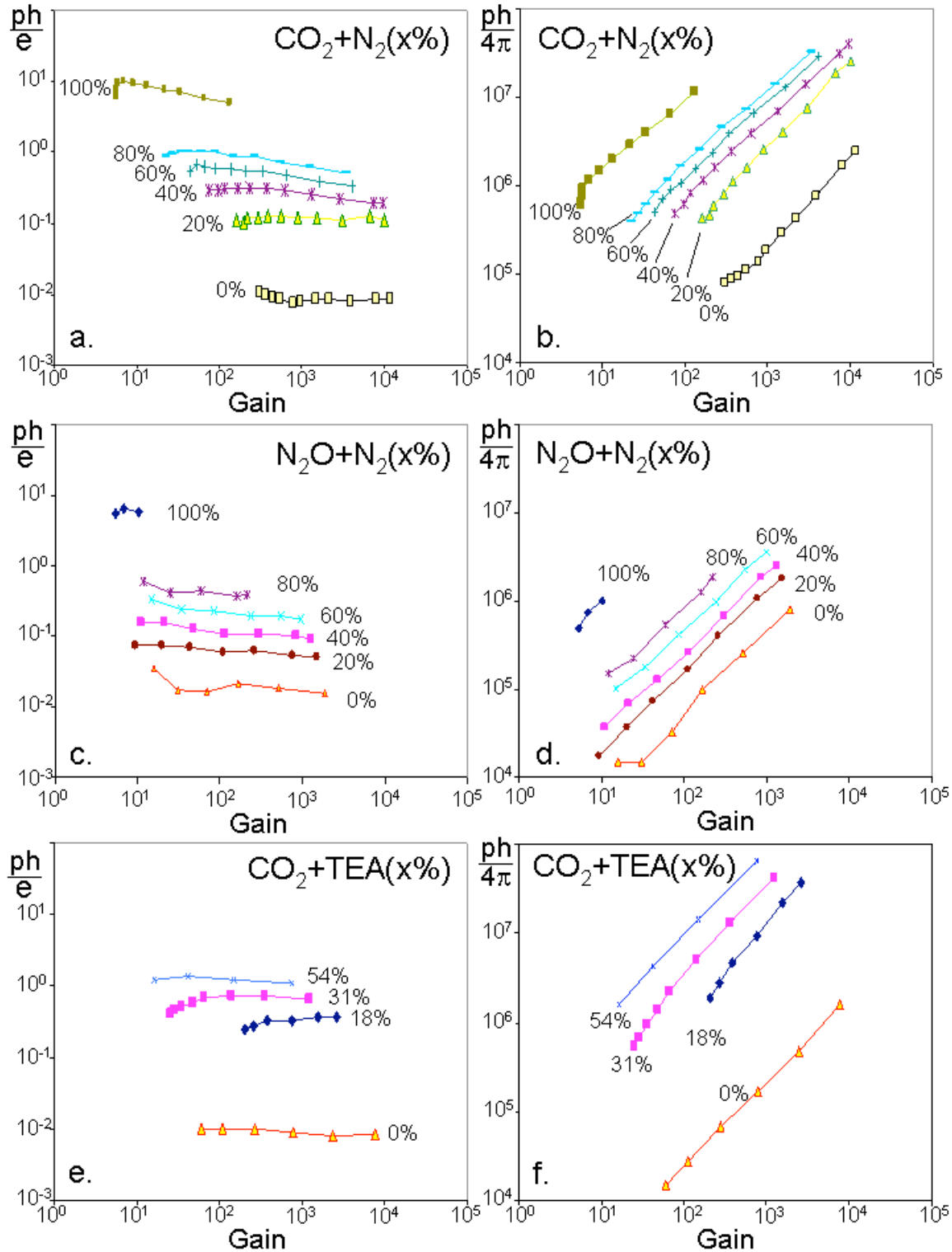


FIG. 5: Electron and photon yields for three gas mixtures, $\text{CO}_2 + \text{N}_2$ (a,b), $\text{N}_2\text{O} + \text{N}_2$ (c,d) and $\text{CO}_2 + \text{TEA}$ (e,f). The total number of emitted photons and the ratio of photons to electrons in the avalanche are plotted as functions of the charge gain. The N_2 and TEA concentrations in the mixtures are shown.

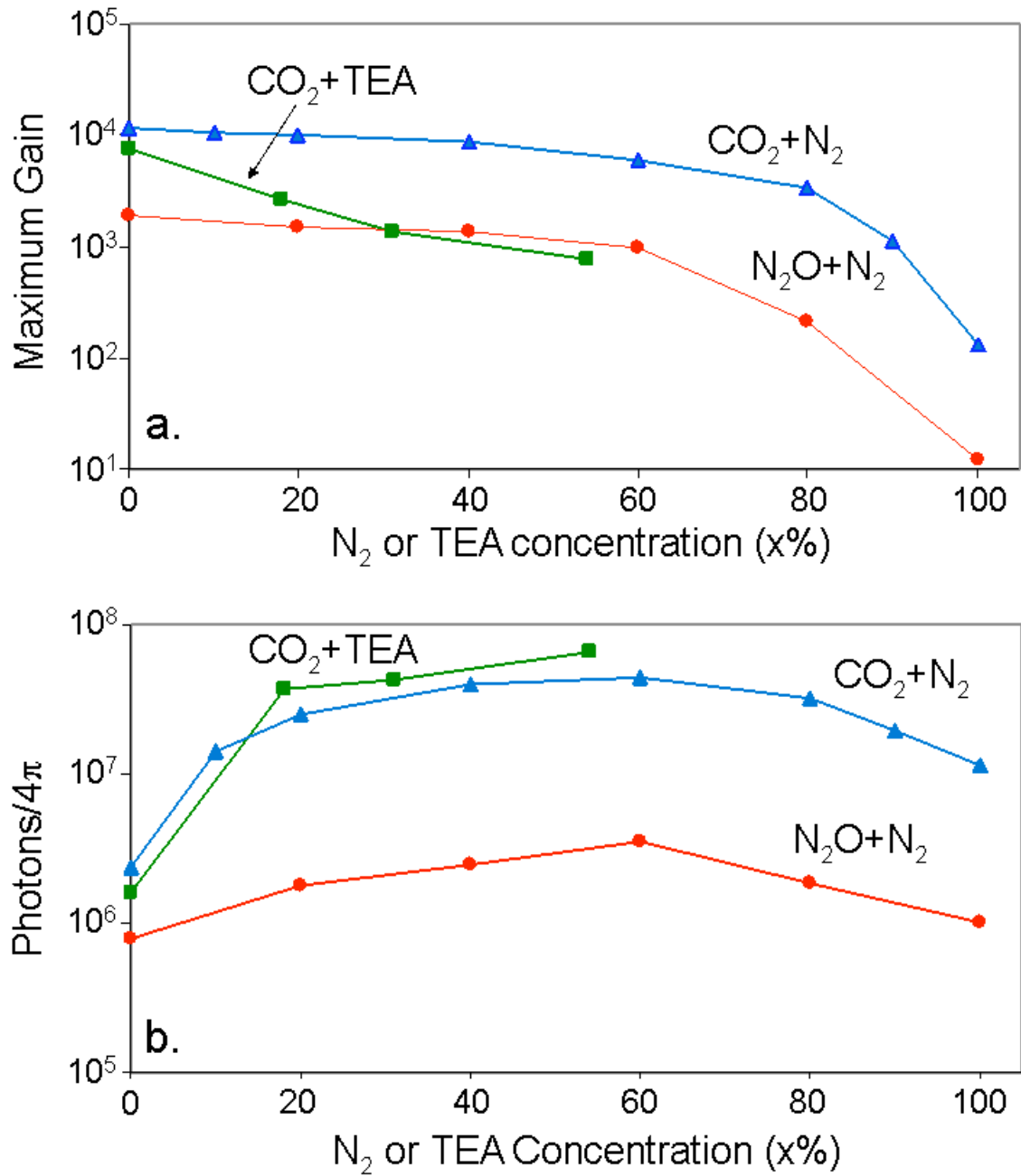


FIG. 6: The maximum gain (a) and the maximum number (b) of emitted photons as a function of concentration of N₂ or TEA. The data presented for CO₂+N₂, N₂O+N₂ and CO₂+TEA.

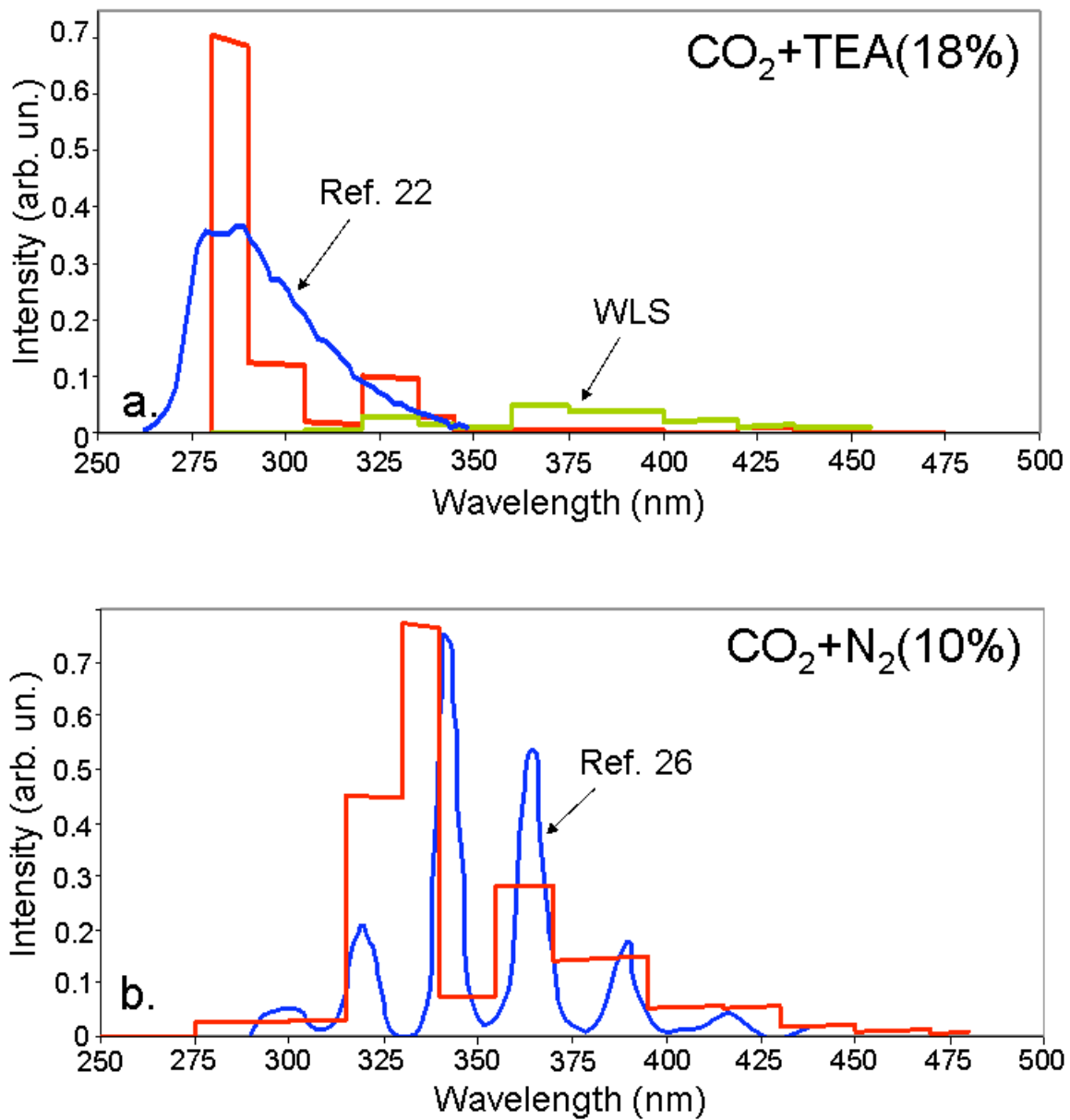


FIG. 7: (a) Emission spectra of CO₂+TEA(18%) and (b) CO₂+N₂(10%) mixtures. The measured emission spectra of TEA and N₂ [22,26] are shown for comparison. The spectrum of CO₂+TEA(18%) measured with an unknown polymer wave-length shifter is also shown.

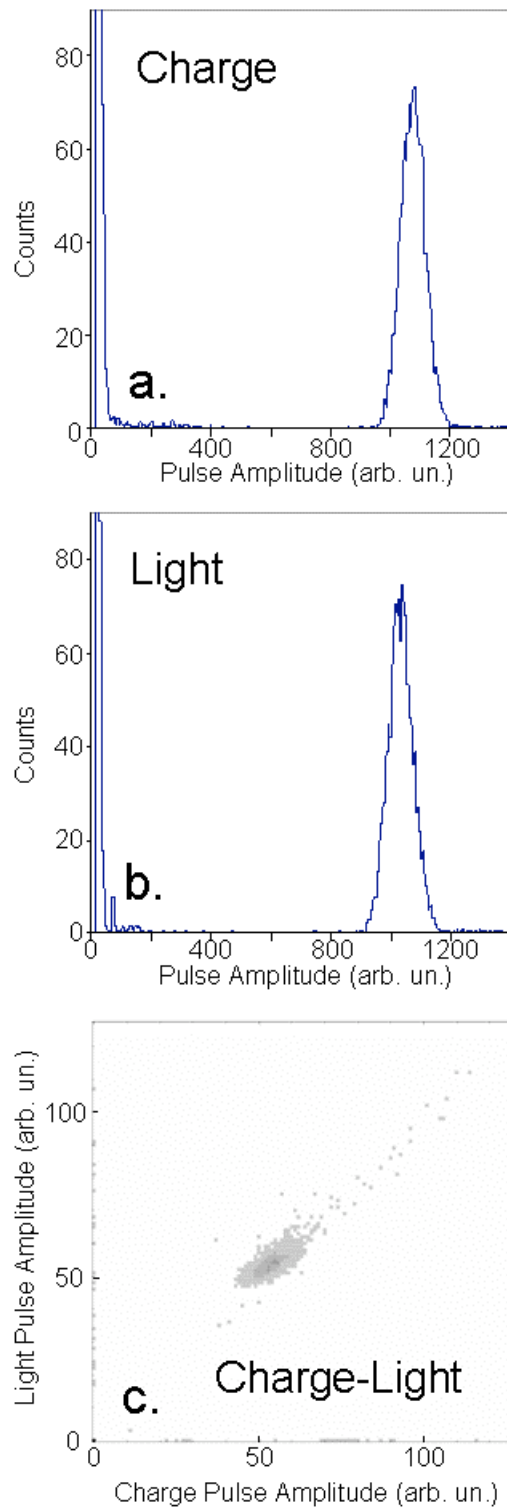


Fig.8. The charge (a) and light (b) distributions obtained with the double-collimated spectroscopic 5.58 MeV alpha-source. The alpha particles were traversing the middle part of the sensitive volume, parallel to the grid electrodes. The light-to-charge correlation plot of the same data is shown in (c). The dark area corresponds to the FWHM of the peak.

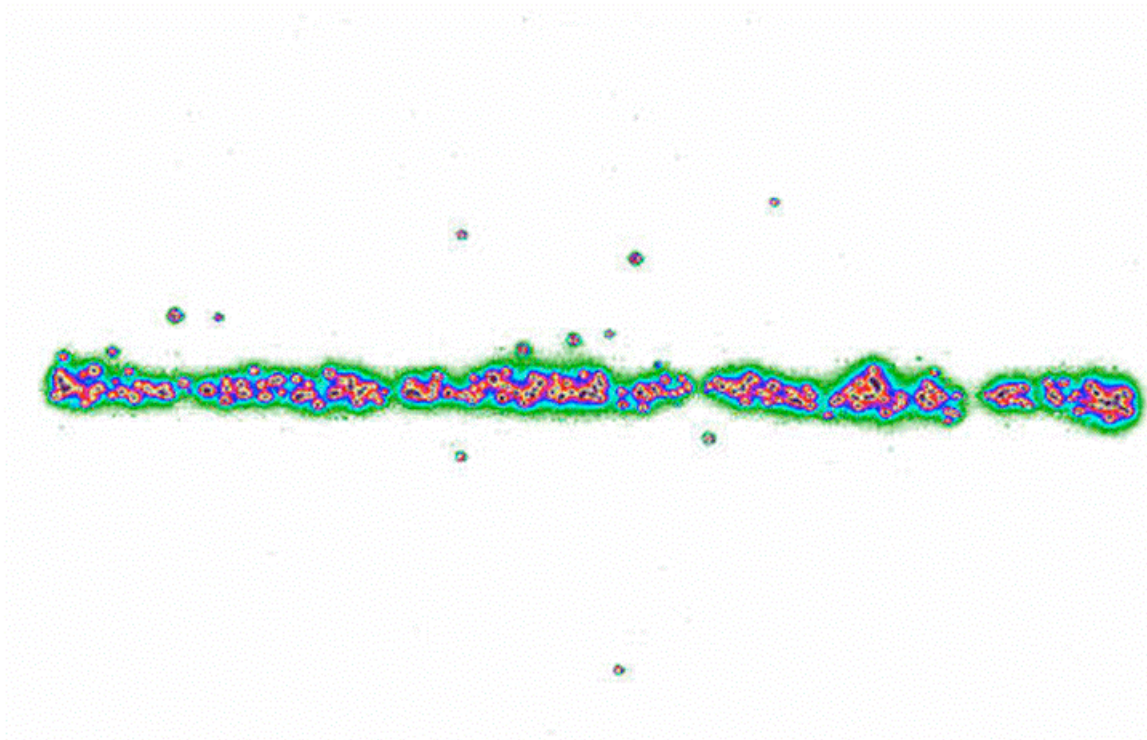


FIG. 9: A typical image of alpha-particle tracks taken with a $\text{CO}_2+\text{N}_2(10\%)$ mixture at 75 Torr. The track length is 90 mm.

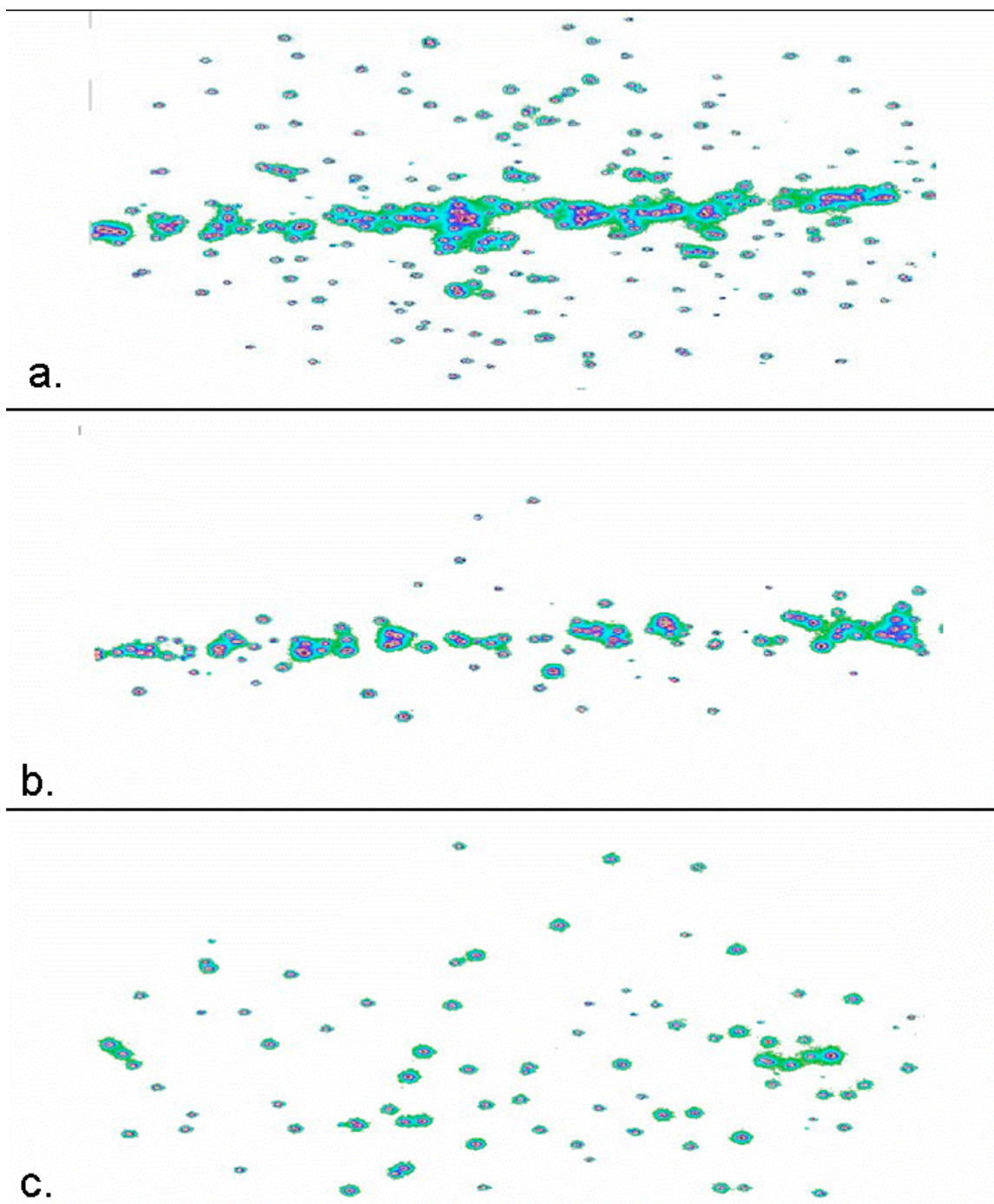


FIG. 10: (a) A typical image of an alpha-particle track with $\text{CO}_2+\text{TEA}(50\%)$ mixture recorded with an ungated image-intensifier. (b) Similar image taken with the image intensifier bias gated by a 400 ns prompt pulse, and (c) a delayed gate on the image intensifier

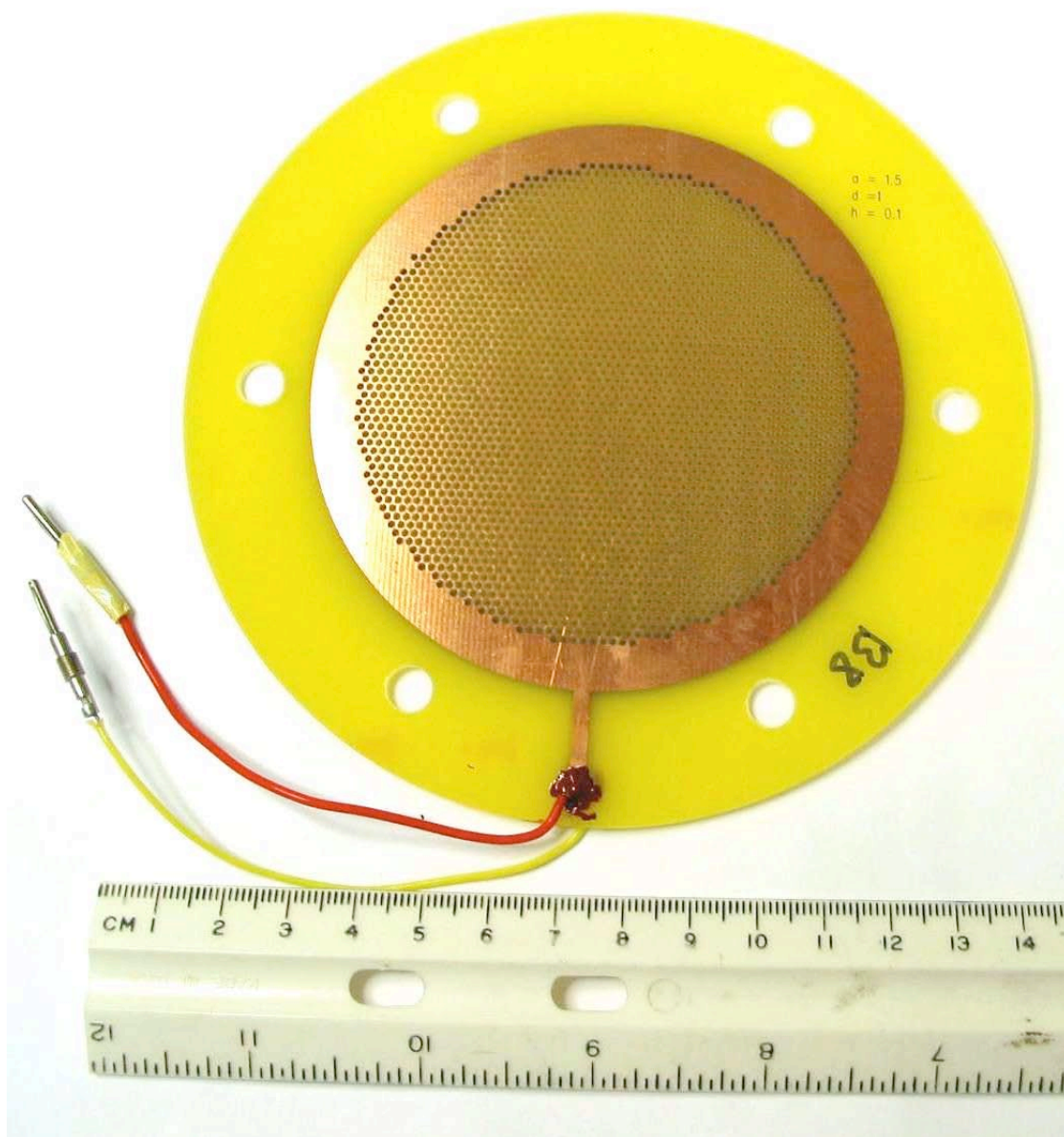


FIG. 11: A photograph of a THGEM used in the measurements.

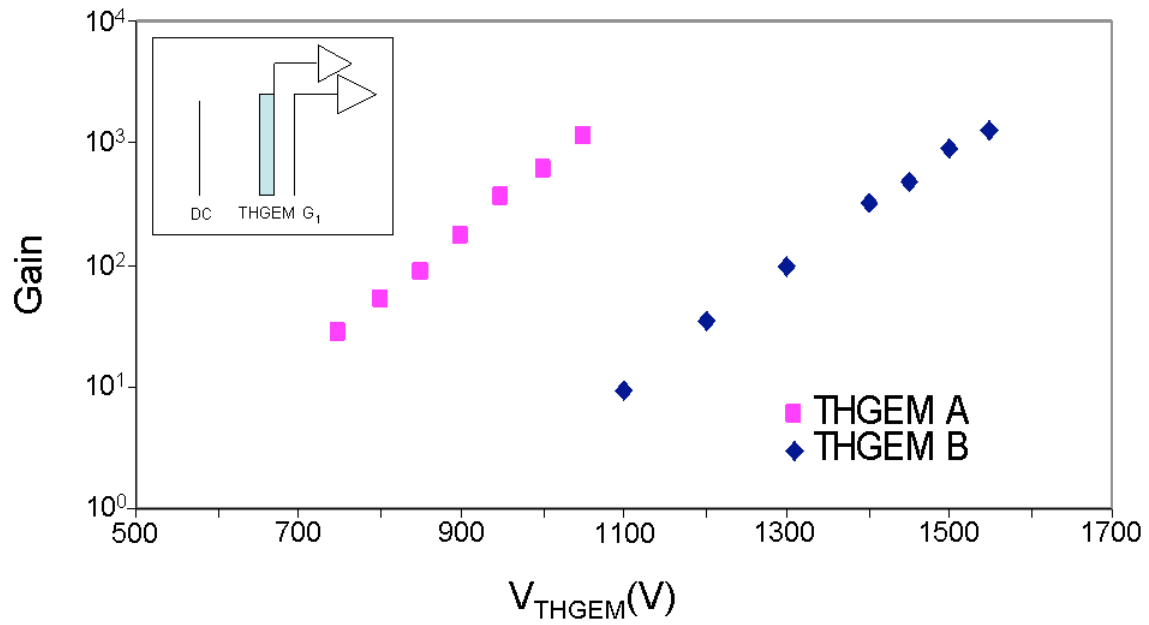


FIG. 12: Dependence of the gain of two different THGEMs (see Table I) on the applied voltage. The measurements were done in a $\text{CO}_2+\text{N}_2(10\%)$ at 75 Torr. A schematic diagram of the electrode configuration is shown in the insert. In these measurements the charge was collected directly on the THGEM's anode.

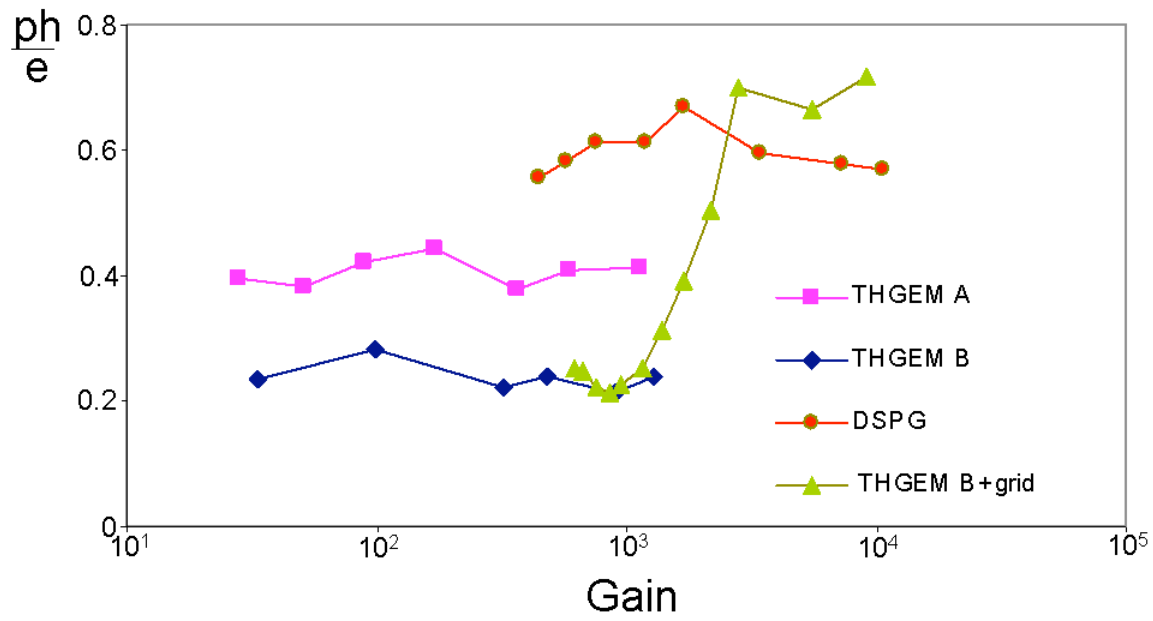


FIG. 13: Photon-to-electron ratio measured with THGEM A, THGEM B (see Table 1), the DSPG and with THGEM B followed by a grid electrode. All measurements were done for a $\text{CO}_2+\text{N}_2(10\%)$ mixture at 75 Torr.

TABLE I: Dimensions of the THGEM electrodes used in this work.

	THGEM A	THGEM B
Thickness (mm)	0.4	1.6
Drilled hole diam. (mm)	0.5	1.0
Etched hole in Cu diam. (mm)	0.7	1.2
Hole pitch (mm)	1.0	1.5
Area (cm ²)	78.5	78.5
Hole diam./Thickness	1.25	0.625